Appl. Phys. B 85, 365–374 (2006)
DOI: 10.1007/s00340-006-2348-1

Applied Physics B
Lasers and Optics

Widely tunable diffraction limited 1000 mW external cavity diode laser in Littman/Metcalf configuration for cavity ring-down spectroscopy

S. STRY[1,✉]
S. THELEN[2]
J. SACHER[1]
D. HALMER[2]
P. HERING[2]
M. MÜRTZ[2]

[1] Sacher Lasertechnik[Group], Rudolf-Breitscheid-Str. 1–5, 35037 Marburg, Germany
[2] Universitätsklinikum Düsseldorf, Institut für Lasermedizin, 40225 Düsseldorf, Germany

Received: 31 March 2006/Revised version: 15 May 2006
Published online: 29 June 2006 •

ABSTRACT We report on recent progress on external cavity diode lasers (ECDL) using a new concept of a Littman/Metcalf configuration. Within this concept one facet of the diode laser chip is used for coupling to a high quality Littman/Metcalf resonator whereas the other side of the diode laser chip emits the output beam. The alignment of the external resonator is independent from the alignment of the output beam and there is no need for any compromise in the alignment. This results in an improved behavior of the external resonator with the benefit of a drastic increase in power and single mode tuning.

We investigated this light source for high resolution spectroscopy in the field of cw-cavity ring-down spectroscopy (CRDS). The monitoring of environmental and medical gases from vehicles or human breath requires a suitable radiation source in the mid-infrared (MIR) between 3 and 5 μm that is frequency stable and can be widely tuned. Since this wavelength cannot be reached via direct emitting room temperature semiconductor lasers, additional techniques like difference frequency generation (DFG) are essential. Tunable difference frequency generation relies on high power, small linewidth, fast tunable, robust laser diode sources with excellent beam quality.

With our new compact, alignment-insensitive and robust ECDL concept, we achieved an output power of 1000 mW and an almost Gaussian shaped beam quality ($M^2 < 1.2$). The coupling efficiency for optical waveguides as well as single mode fibers exceeds 70%. The wavelength is widely tunable within the tuning range of 20 nm via remote control. This laser system operates longitudinally in single mode with a mode-hop free tuning range of more than 150 GHz without current compensation and a side-mode-suppression better than 50 dB. This concept is currently realized within the wavelength regime between 750 and 1080 nm.

Our high powered Littman/Metcalf laser system was part of a MIR-light source which utilizes DFG in periodically poled lithium niobate (PPLN) crystals. At the wavelength of 3.3 μm we were able to achieve a high-resolution absorption spectrum of water with four different isotoplogues of H_2O components. This application clearly demonstrates the suitability of this laser for high-precision measurements.

PACS 07.57.Ty; 42.55.Px; 42.62.Fi

✉ Fax: +49-6421-305-299, E-mail: sandra.stry@sacher-laser.com

1 Introduction

Using high-power laser diodes directly in an external cavity configuration combines the high power of these diodes with the advantages of the external cavity: a narrow linewidth lower than one MHz and good wavelength tunability [1] of more than 20 nm, in combination with ease of use and small dimensions. Within a 'conventional' external resonator concept [1], only one side of the diode is useable. One side of the diode has a high reflectivity coating (HR) while the other side is anti-reflection coated (AR). In the Littrow configuration the emitted light from the AR coated side of the laser diode illuminates a low efficiency grating. The −1st order is reflected back into the resonator and the 0th order is used as the output beam. In the Littman/Metcalf configuration, shown in Fig. 1, the −1st order is reflected to a mirror in such a way that the HR coated facet and the mirror define the resonator. Such a 'conventional' external cavity diode laser (ECDL) design has severe drawbacks: In order to achieve high output power, there is the need for operating the grating in low efficiency mode which means the grating efficiency should be in the range of 10% to 40% depending on the resonator configuration. Due to the fact that the light passes the grating twice within the Littman configuration the efficiency of the −1st order of the grating must be twice as high as in the Littrow configuration. Most gratings have a high effi-

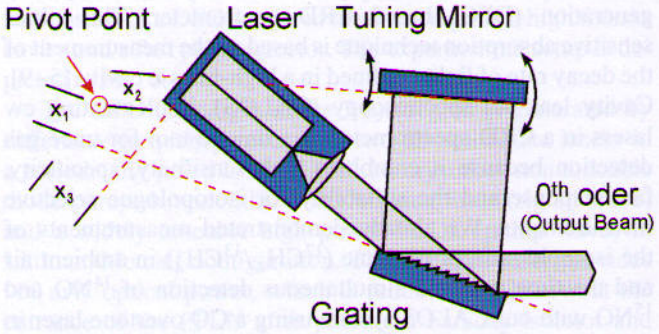

FIGURE 1 Principle of the ECDL in Littman/Metcalf configuration. The external cavity is defined by a reflecting element and the front facet of the laser diode. A diffraction grating inside the cavity is used for the wavelength selection. The −1st order of the grating is reflected back into the diode. The 0th diffraction order of the grating is used as the output beam. There is no independent alignment of resonator and output beam

ciency of 80–90% for *p*-polarized light and a low efficiency of 10–20% for *s*-polarized light. To get the low efficiency in the −1st order the diode light within the resonator must be *s*-polarized. A standard antireflection coated diode has a polarization ratio of 1 : 50. As a result there are non-negligible contributions of the 'other' polarization within the feedback loop inside the external resonator. This results in a poor polarization ratio between TE and TM emission for ECDLs with high output power. Furthermore, this non-optimized resonator quality leads to a poor side mode suppression in the order of 40 dB. Another drawback of the Littrow design is the beam walk of the out-coupled laser beam. During a 30 GHz wavelength scan, a parallel shift in the order of up to 10 μm appears, even with a beam steering mirror attached to the grating. This causes serious problems in terms of stability, e.g., in case of coupling to a single mode fiber or to amplification stages. Within the Littman configuration where the high reflective mirror is rotated for wavelength tuning there is no beam walk present.

For designing a high power ECDL, the best configuration is the Littman/Metcalf configuration with an optimized feedback from the diffraction grating. As a result, it is not possible to use the 0th order as laser output any more.

With a special mounting scheme for the applied laser diodes both facets are accessible. An increase of the output power and the total performance of the Littman/Metcalf laser can be achieved by using a high efficiency grating and by coupling the light out of the rear facet of the laser diode. With this approach, we are able to increase the output power to more than 1000 mW. Our external cavity semiconductor laser system is designed to achieve a maximum mechanical stability and maximum output power, in addition to a small linewidth and good tunability. The laser source of the ECDL is a commercial laser diode where one of the facets is antireflection coated, which suppresses the reflectivity typically below 10^{-4}. These types of diodes are also usable within a Littrow configuration to get higher output power [2–4].

The presented results were measured in the wavelength regime of 800 nm. We also tested other wavelengths regimes at 770 nm, 830 nm, 850 nm, 920 nm, 960 nm, 1010 nm and 1060 nm. Further wavelength regions are under investigation. These results will be presented elsewhere.

The capability of our motorized high power Littman/Metcalf ECDL was demonstrated within a difference frequency generation (DFG) based CRD-spectrometer. This ultrasensitive absorption technique is based on the measurement of the decay rate of light confined in a high-finesse cavity [5–9]. Cavity leak-out spectroscopy (CALOS), implementing cw lasers in a CRD-spectrometer, is a unique tool for trace gas detection because it combines high sensitivity, specificity, fast response and the suitability for isotopologue selective measurements. We already demonstrated measurements of the isotopic ratio of methane ($^{12}CH_4/^{13}CH_4$) in ambient air and the time resolved simultaneous detection of ^{14}NO and ^{15}NO with our CALOS system using a CO overtone laser in the 3 μm region and a CO laser in the 5 μm region respectively [10, 11]. In order to develop a portable spectrometer suited for environmental and medical applications one needs a compact setup. The bulky CO overtone laser does not match this prerequisite. For that reason we developed a portable CALOS system, using a DFG laser source at 3 μm [7, 12]. The new ECDL in Littman/Metcalf configuration was used as a light source within the DFG laser system. With our tuneable ECDL and a non tuneable Nd:YAG laser system such a DFG laser source is tuneable between 3125 nm and 3485 nm (2870–3200 cm^{-1}). The wavelength regime around 3 μm is ideally suited for this measurement technique since various atmospheric or medical relevant molecules show a characteristic fingerprint absorption. The combination of a compact light source with a suitable CRDS set-up results in a portable trace-gas analyzer with high sensitivity and high specificity which is required for various environmental and medical applications [13].

The isotopologue selective analysis of water vapor is of considerable interest in a variety of environmental applications, among them atmospheric measurements [14] and plant physiology [15]. We measured a water spectrum around 2997 cm^{-1} where the different isotopologues of water are visible within the spectrum. This shows the excellent tunability behaviour of our ECDL as well as its perfect brilliance.

2 External resonator configuration

2.1 *Setup of the high power Littman/Metcalf diode laser*

With a special mounting scheme of diodes both facets are accessible so that one facet can be used as the output beam and the other side is coupled to the external resonator. Figure 2 shows a schematic interior view of our tunable external cavity in Littman configuration. This new design uses the rear facet of the diode laser chip for coupling the laser light out of the system. This has a number of advantages: We are able to design a high quality external cavity without any compromises. The polarization ratio is now improved by the cavity and typical values are well above 1 : 200. The side mode suppression of the laser system is improved with typical values of 55 dB and better. Also the total tuning range as well as the mode-hop free tuning range are drastically improved and a beam walk is no longer present while changing the wavelength through adjusting the grating angle. An in-

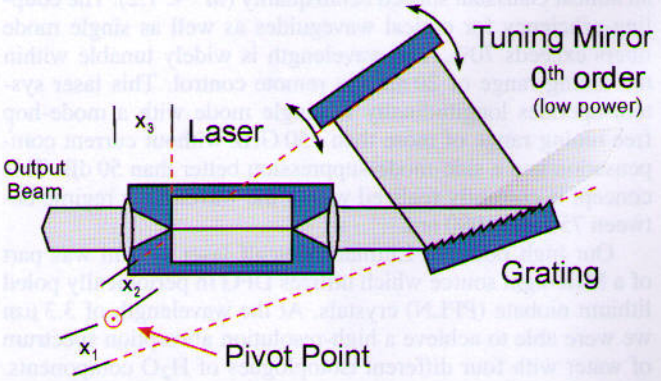

FIGURE 2 Principle of the new Littman/Metcalf configuration. The external cavity is defined by a reflecting element and the front facet of the laser diode. A diffraction grating inside the cavity is used for the wavelength selection. The −1st order of the grating is reflected back into the diode. Only a small part is coupled out via the 0th diffraction order of the grating. The main part of the laser light coming from the rear facet of the diode is collimated with a set of lenses

crease of the output power and the total performance of the Littman/Metcalf laser is achieved by using a high efficiency grating.

In order to tune such a laser modehop-free, it is required to synchronize the grating defined wavelength with the cavity. We realized the synchronization between grating defined and cavity defined wavelength by simply rotating the back reflecting mirror around the pivot point. The adjustment of the pivot point is done during the wavelength scanning operation of our Littman/Metcalf laser [16]. Due to this special method, we are able to ensure the best mode-hop free tuning behavior. The wavelength selectivity of the grating forces the laser to oscillate in one single longitudinal mode. The coarse tuning (> 20 nm) can be done with a precision of 1 GHz using a stepper motor; fine tuning with a precision of 100 kHz using the piezoelectric transducer. For high speed locking techniques a high frequency bias tee is included in the laser head.

Furthermore, the collimation inside the resonator is independent from the collimation of the output beam. This has the significant advantage that the collimation within the resonator can be optimized for best illumination of the grating whereas the collimation lens for the output beam can be optimized for the requirements of the experiment the laser will be used for. With tapered diodes it is also possible to realize high power laser systems with a Littman/Metcalf configuration with an output power of up to 1000 mW. This makes the system a good replacement of common master-slave laser systems [17]. The combination of the Littman/Metcalf resonator concept with this new diode generation leads to a widely tunable laser system with maximum frequency stability and extremely small linewidth with maximum output power. The resonator quality is extremely improved, which results in a higher sidemode suppression and a better tuning behavior. With this resonator concept an automated wavelength change with a motor system for coarse tuning and with piezo actuator for fine tuning is also possible.

Here we demonstrate a novel external cavity diode laser (ECDL) employing Fabry–Pérot diodes as well as high power tapered laser diodes within the Littman/Metcalf configuration with computer controlled wavelength change over more than 20 nm. This system greatly simplifies the experimental setup while increasing the available laser power up to 1 W with all the advantages of a Littman/Metcalf design.

2.2 *Effects of the resonator feedback on the power-injection curve*

One of the most obvious effects of an external resonator on diode lasers is the effect on the threshold current and on the quantum efficiency of the diode laser as seen in the power curves of the next section of this publication. For an understanding of this effect, one needs to start with the rate equation description of semiconductor diode lasers for the dynamics of the laser power $S(t)$ and the carrier density $N(t)$ as they are given in [18, 19]

$$\frac{\mathrm{d}n}{\mathrm{d}t} = J - \frac{N}{\tau_n} - \frac{\mathrm{d}g}{\mathrm{d}N}(N - N_{\mathrm{th}})S, \tag{1}$$

$$\frac{\mathrm{d}S}{\mathrm{d}t} = \Gamma_{\mathrm{conf}}\frac{\mathrm{d}g}{\mathrm{d}N}(N - N_{\mathrm{th}})S - \frac{S}{\tau_s} + \beta\Gamma_{\mathrm{conf}}\frac{N}{\tau_n}. \tag{2}$$

J is the normalized pump current, which is determined by the injection current and the active volume of the laser, τ_n is the carrier lifetime, $\mathrm{d}g/\mathrm{d}N$ is the differential gain G_N, and N_{th} is the carrier density at threshold. Γ_{conf} is the confinement factor which accounts the fact that only a part of the optical mode is in the active volume. τ_s is the photon lifetime and β is the fraction of the spontaneous emission which is coupled into the lasing mode.

The photon decay rate $1/\tau_s$ is separated into two terms, one describing the internal losses, the second one describing the distribution of the feedback of the external resonator.

$$\frac{1}{\tau_s} = \Gamma - \kappa, \tag{3}$$

where Γ is the modified photon decay rate without coating and κ the variation of the photon decay rate due to the feedback of the external resonator. With this approach, we obtain a simple expressions for the threshold current density J_{th} as well as the laser output power S as a function of the feedback factor κ:

$$J_{\mathrm{th}} = \frac{N_{\mathrm{th}}}{\tau_n} - \frac{\kappa}{\tau_n G_N}. \tag{4}$$

The threshold current J_{th} linearly decreases with an increasing feedback rate κ of the external cavity. β is of the order of 10^{-4} which means $(1 - \beta) \simeq 1$. Therefore the output power S can be written as:

$$S = \Gamma_{\mathrm{conf}}\frac{J - \dfrac{N_{\mathrm{th}}}{\tau_n}}{\Gamma - \kappa}. \tag{5}$$

The output power S of the laser system increases within a nonlinear scaling on the feedback rate κ. High values for κ indicate a higher reflectivity of the external resonator mirrors which also leads to a better side-mode suppression. Equations (4) and (5) describe most aspects of the steady state description of external cavity diode lasers. Due to these two equations, the threshold current of an ECDL with higher feedback rate should be reduced and the output power should be increased with the new concept.

3 Setup of the cavity leak-out spectrometer

The experimental set-up of the CALO-spectrometer consists of a DFG source in the 3 μm region, a high finesse cavity and a fast photodetector. The experimental setup is depicted in Fig. 3.

The DFG laser light in the 3 μm region is generated by difference-frequency mixing of two all solid-state lasers in a periodically poled $LiNbO_3$ (PPLN) crystal: A non tuneable diode-pumped monolithic Nd:YAG ring laser (signal wave) and a widely tuneable high power ECDL (pump wave) in Littman/Metcalf configuration. The Nd:YAG laser provides 900 mW optical power, which is reduced to 820 mW at the entrance of the PPLN after passing a Faraday isolator and an electro–optical modulator (EOM). The high power ECDL, being widely tuneable between 793 nm and 815 nm, generates a maximum output power of 580 mW, which is coupled into a polarization maintaining single mode fiber. The resulting output beam has a maximum power of 280 mW and the

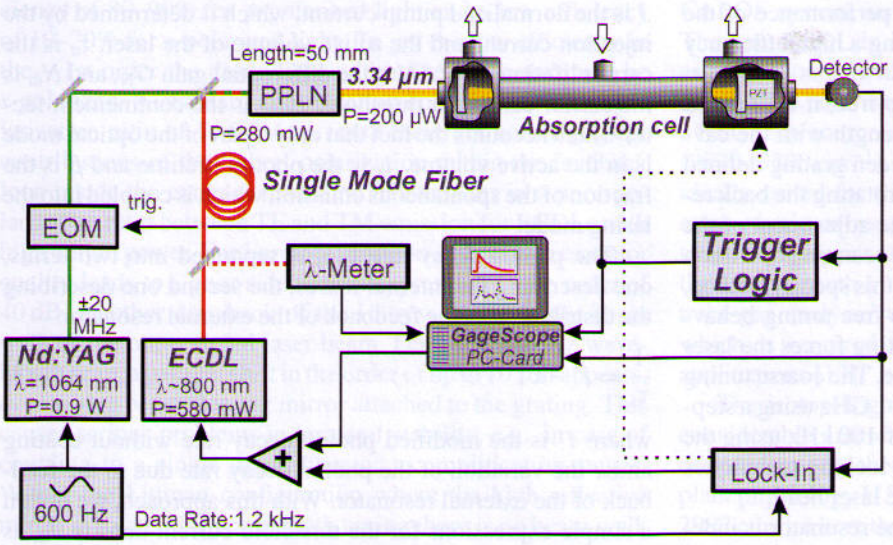

FIGURE 3 Experimental setup of the CALO spectrometer. The DFG laser light is coupled into the high finesse cavity (absorption cell); the decay of the radiation is measured after turning off the laser. EOM: electro–optical modulator, ECDL: external cavity diode laser, PPLN: periodically poled lithium niobate, PZT: piezoceramic transducer

M^2 value of 1.05 indicates a nearly perfect Gaussian shape. Both laser beams are horizontally polarized and focused into the PPLN crystal with beam waists of 61.5 µm and 39.4 µm for the signal wave and the pump wave, respectively. The PPLN crystal is 5 cm long and AR-coated on both sides. The z-cut crystal consists of 21 stripes, each 0.9 by 0.5 mm wide, with different poling periods ranging from 20.6 µm to 22.6 µm in 0.1 µm steps. The PPLN crystal is fixed inside an electrically heated oven stabilizing the crystal temperature between 20 and 120 °C with an accuracy of 0.03 °C. The oven is mounted on a 6-axis translation and rotation stage, thus the appropriate poling period can be selected to generate the DFG laser beam with a frequency between 2870 cm^{-1} and 3200 cm^{-1}. Pump and signal wave are separated behind the PPLN by a dichroic mirror and the pump wave is fed into a wavemeter where the wavelength of the diode laser is determined with a precision of ±200 MHz.

The DFG laser beam emanating from the crystal is used to excite the fundamental transverse mode (TEM_{00}) of the cavity, a high finesse resonator with plano-concave mirrors (reflectivity 99.985%). Due to the high reflectivity of the cavity mirrors the instantaneous linewidth of the cavity modes is 14 kHz and the effective absorption path length inside the cavity reaches 3.4 km. The mirrors are set at a distance of 51 cm, resulting in a free spectral range of 294 MHz.

The DFG laser frequency is sinusoidally modulated by modulating the Nd:YAG laser frequency through a piezoceramic transducer (modulation frequency: 600 Hz, modulation depth: ±20 MHz). Thus the stabilization of the DFG laser frequency to the cavity resonance can be realized by a standard 1f-lock-in technique. The stabilization is performed by controlling the frequency of the ECDL via a piezoceramic transducer.

The DFG power is injected into the cavity every time the laser frequency is in coincidence with the cavity resonance. Each time the transmitted laser power indicates an optimum match of laser frequency and cavity mode, the DFG laser power is turned off within 500 ns by means of an EOM. The subsequent single-exponential decay of the laser power is measured by a LN_2-cooled InSb photodetector. The decay signals are preamplified with a transimpedance amplifier

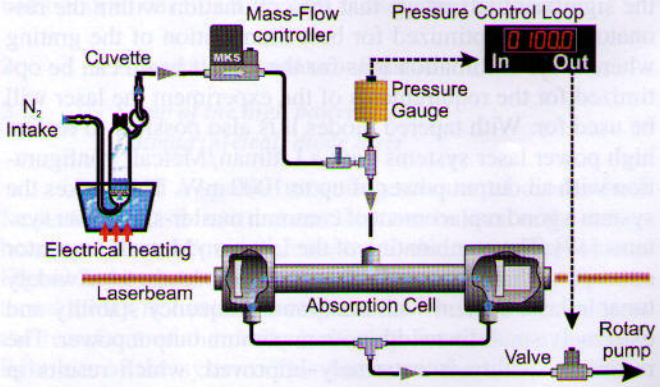

FIGURE 4 Schematic of the gas handling setup. The cavity (absorption cell) is flushed with a sample gas mixture consisting of N_2 that is saturated with water vapor

(10^5 V/A, 840 kHz bandwidth) and obtained by a 50 MHz 12-bit analog-to-digital data-acquisition-card in a personal computer. The decay time (1/e time) of each decay signal is calculated in real time by a very fast exponential fitting algorithm [20] and averaged over a preset number of decays. The decay time τ of the cavity filled with a gas sample is shorter than the decay time τ_0 of the evacuated cavity due to the additional absorption loss $\alpha(\lambda)$. With c as speed of light and λ as DFG wavelength $\alpha(\lambda)$ can be calculated via (6):

$$\alpha(\lambda) = \frac{1}{c}\left(\frac{1}{\tau(\lambda)} - \frac{1}{\tau_0(\lambda)}\right) . \qquad (6)$$

The gas handling system is depicted in Fig. 4. A glass cuvette filled with distilled water is set in a basin containing undistilled water heated to a temperature of 70 °C. The distilled water inside the cuvette is evaporated saturating the grade 5 nitrogen gas which is flushed through the cuvette. The gas mixture consisting of nitrogen, and saturated water vapor is sucked into the gas system by means of a rotary pump. The flow rate is controlled by an electronic mass flow controller. The gas pressure inside the absorption cell is stabilized independently of the mass flow by a pressure control loop. The corresponding gas system is described in more detail in [21].

4 Results and discussion

We demonstrate the suitability of our high power Littman/Metcalf concept with two different types of diodes. For the power range of 150 mW we use normal Fabry–Pérot (FP) diodes where we optimize the output reflectivity especially for this concept. To reach power levels of up to 1000 mW, we use tapered (TA) diodes within this concept. Both systems were designed with a stepper motor and a piezoelectric transducer. In this section we report our investigations of the most important characteristics of such a laser system with an external resonator. We discuss the output power, spatial beam quality, the sidemode suppression, linewidth, and tuning behavior of our high power laser. Furthermore we performed a high resolution absorption experiment (CRDS), which shows the excellent suitability of such high power ECDL for this kind of application.

4.1 *Power characteristic*

The improvement our high power Littman/Metcalf configuration is shown by the measurement of the laser output power vs. laser injection current. In Fig. 5 the ECDL power curves for two different types of diodes after antireflection coating of the inner facet is shown. The antireflection coating in the order of 10^{-4}–10^{-5} is necessary to prevent mode competition between the internal diode modes and the external resonator modes. For both types of diodes (FP-diodes and TA-diodes) the power curves for the lowest, center and highest wavelength were measured. Due to the lower gain factor at the border of the diode gain profile the measured threshold current there is much higher than for the center wavelength.

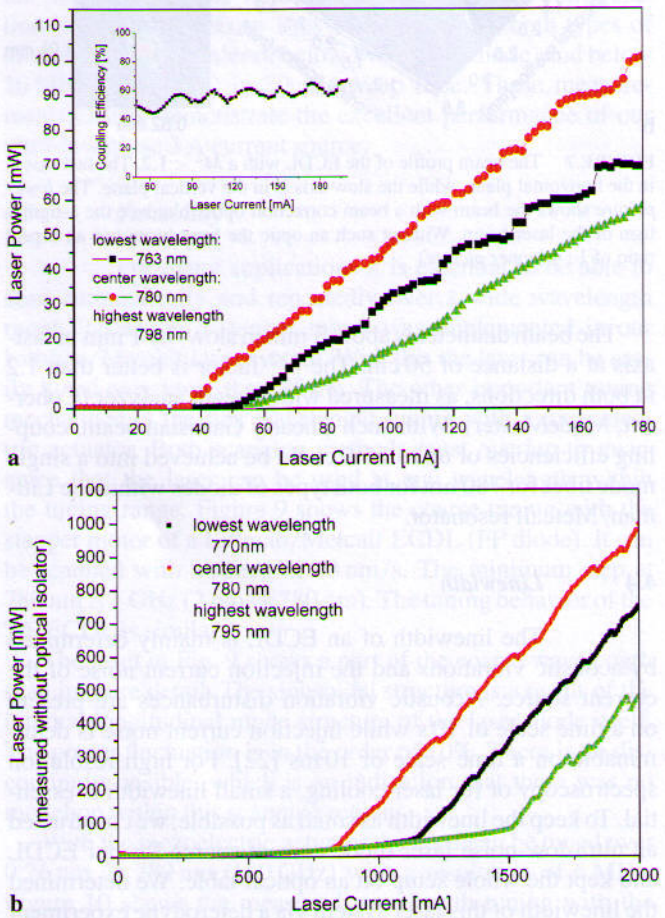

FIGURE 5 Power characteristic of the ECDL diode laser current for the lowest, center and highest laser wavelength. The *upper picture* shows the power reached with a FP-diode (**a**), the *lower picture* the achieved power with a TA-diode (**b**) in the Littman/Metcalf configuration. The *inset* shows the reached coupling efficiency vs. laser diode current for the center wavelength

We tested the same type of FP-diode delivered from the same manufacturer with different types of external resonator configurations. Within a standard Littrow configuration, a grating efficiency of 10%–20%, in the old Littman/Metcalf concept, where the 0th order of the grating is used as laser output, a grating efficiency of the −1st order of 20%–40% is used depending on the laser wavelength and the diode performance. The higher efficiency of the grating inside the Littman/Metcalf is necessary because of the double passing of the light. For both configurations the measured threshold current for a 780 nm FP-diode is 50 mA. Within the new Littman/Metcalf ECDL the threshold is only 29 mA @ 780 nm as shown in Fig. 5a. This is due to the better grating efficiency of 80% in the −1st order and the fact that the second facet of the diode is used as laser output. With the same type of FP-diode we achieved a maximum output power of more than 100 mW after an optical isolator at 780 nm. This demonstrates that we were able to combine high output power with an improved cavity feedback. The better resonator quality results in a better single mode tuning behavior, see Sect. 4.5. The inset of Fig. 5a shows the reached coupling efficiency. We obtained a constant coupling efficiency of more than 50% which is an indicator for the high spatial mode stability while changing the laser current.

The use of tapered diodes is only possible with this new Littman/Metcalf concept. The waveguide side of the tapered diode is oriented to the external resonator. Therefore the light filtered by the external resonator is amplified in the tapered structure. Due to the high cavity feedback, the single-mode tuning of the laser is also improved compared to the old configuration.

The improvement of the laser resonator is also visible in the better spectral behavior which means larger coarse tuning range as well as better side mode suppression.

4.2 *Spectral behavior*

The total available tuning range of a laser diode in an external resonator is determined by its gain profile and the resonator configuration. Using a very good antireflection coated diode, one can grating-tune the ECDL in Littman-Metcalf in the old configuration (grating efficiency −1st order: 40%) from 765 nm to 785 nm with an output power of up to 20 mW (standard FP diode). Using the new concept (grating with an efficiency of 80%), one can drastically enlarge the coarse tuning range from 763 nm to 798 nm. The improvement is larger for higher wavelengths. This is due to the band structure of a direct semiconductor. Figure 6 shows the side mode suppression for both types of diodes (FP- and TA-diode), which we could achieve at lowest, center and highest wavelength, analyzed with an optical grating spectrom-

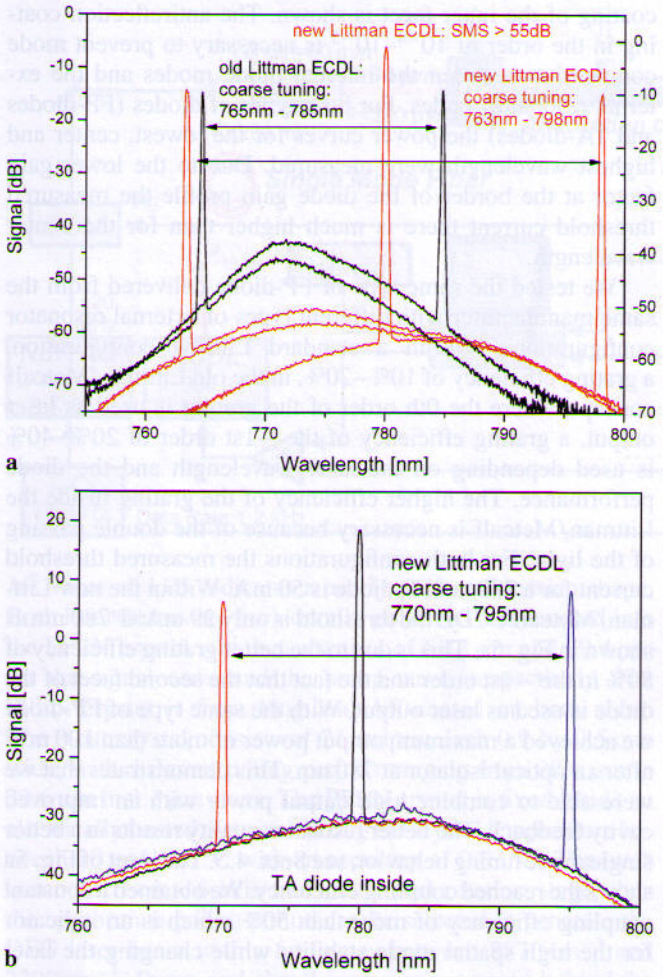

FIGURE 6 Spectrum of our Littman/Metcalf ECDL: *upper picture* FP-diode: side mode suppression of 50 dB (**a**); output power of 150 mW, *lower picture* TA-diode: side mode suppression of 45 dB; output power of 750 mW (**b**)

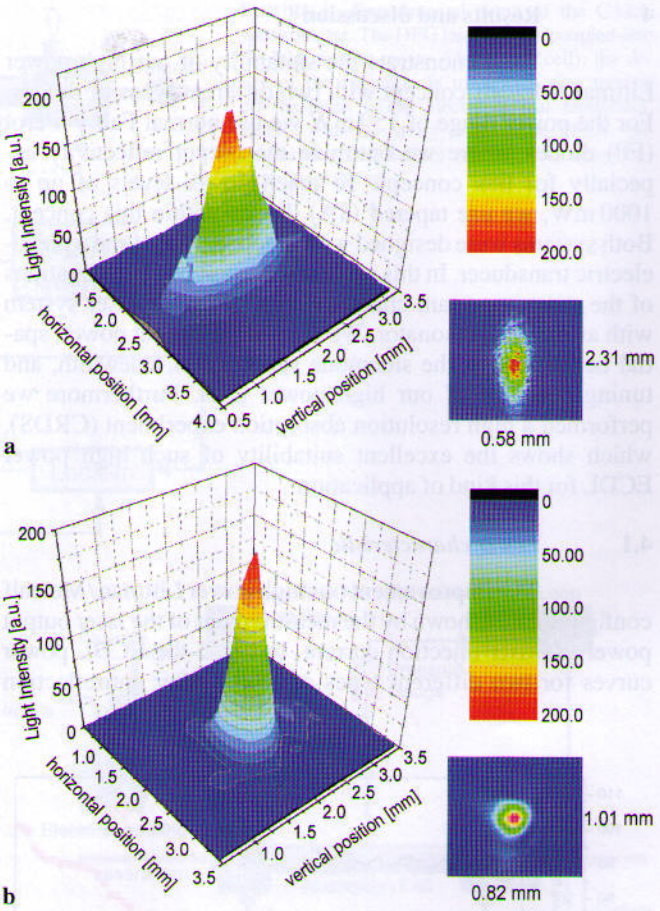

FIGURE 7 The beam profile of the ECDL with a $M^2 < 1.2$. The fast axis is in the horizontal plane, while the slow axis is in the vertical plane. The *lower picture* shows the beam with a beam correction optic to reduce the astigmatism of the laser beam. Without such an optic the laser beam has an aspect ratio of 1 : 4 (*upper picture*)

eter (ANDO AQ6315A). For the FP-diode in the new Littman/Metcalf concept the sidemode suppression is larger than 55 dB, which is 10 dB higher than in the old design. The sidemode suppression of the new concept with a TA-diode inside is only 48 dB. This lower value is due to the amplifier stage within the TA-diode. We measured that more than 95% of the emitted power is within the laser line and only about 5% is due to spontaneous emission background, which can be decreased further by using an optical filter.

4.3 *Beam profile*

The beam profile of the ECDL output light was analyzed by a CCD camera (Coherent, LaserCam II – 1/2). The collimation within the resonator can be aligned independently from the output beam. This gives us the possibility to use different optics for the output beam, e.g., we can implement beam correction optics to produce a circular beam profile or a focus at a particular distance from the laser head. Figure 7 illustrates the beam profile of the high power laser ECDL in Littman/Metcalf configuration with and without beam correction optic. Without such an optic, which is used to compensate the astigmatism of the output beam, the aspect ratio is 1 : 4.

The beam diameter is about 3 mm in slow- by 1 mm in fast-axis at a distance of 50 cm. The M^2 factor is better than 1.2 in both directions, as measured with a beam analyzer (Coherent, ModeMaster). With such a nearly Gaussian beam, coupling efficiencies of up to 75% could be achieved into a single mode fiber for 780 nm for both types of diodes within the Littman/Metcalf resonator.

4.4 *Linewidth*

The linewidth of an ECDL is mainly determined by acoustic vibrations and the injection current noise of the current source. Acoustic vibration disturbances are present on a time scale of 10 s while injection current noise is determinable on a time scale of 10 ms [22]. For high resolution spectroscopy or for laser cooling, a small linewidth is essential. To keep the linewidth as small as possible, we constructed an ultra-low-noise laser diode current source for our ECDL and kept the whole setup on an optical table. We determined the linewidth of this laser system via a heterodyne experiment with two Littman/Metcalf laser systems.

In the lower part of Fig. 8 the beat signals of three independent measurements are shown. These measurements were linearized (upper part) to determine the FWHM linewidth. Tak-

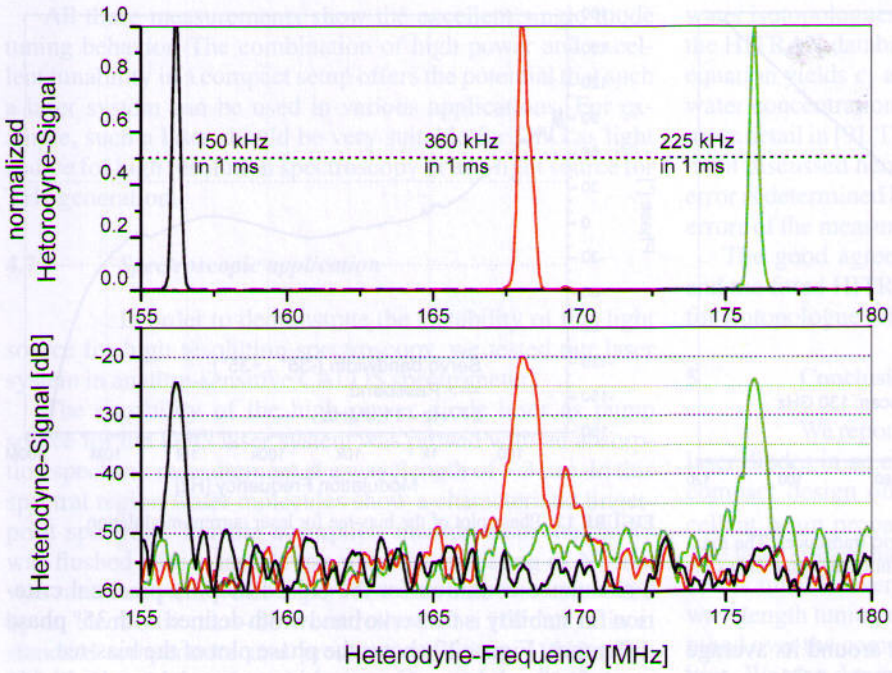

FIGURE 8 Linewidth in 1 ms sweep time: 200 kHz. Three independent scans are shown here. Resolution bandwidth: 100 kHz

ing into account that the value is a result for both linewidths, the linewidth for one ECDL in Littman/Metcalf configuration is about 100 kHz in 1 ms sweep time (for both types of diodes) and in the order of below 1 MHz (FP diode) and below 10 MHz (TA diode) in 20 ms sweep time. These measurements clearly demonstrate the excellent performance of our ultra-low noise 3 A current source.

4.5 *Tunability*

For many applications it is essential to be able to scan automatically and repeatedly over a wide wavelength range. Therefore a stepper motor was implemented in our Littman/Metcalf laser system. With this the laser can be easily tuned over more than 25 nm. The other important tuning mechanism is the fine wavelength tuning with a piezoelectric actuator. Both scanning methods must overlap to guarantee that the laser can be used at any wavelength within the tuning range. Figure 9 shows the coarse tuning with the stepper motor of a Littman/Metcalf ECDL (FP diode). It can be scanned with a speed of 10 nm/s. The minimum step at 780 nm is 1 GHz (2 pm @ 780 nm). The tuning behavior of the TA-ECDL is similar.

The inset in Fig. 9 shows a part of the coarse wavelength scan in more detail. The sinusoidal structure is a result of the internal longitudinal mode structure of the laser diode itself. The power fluctuation is in the order of 10%. There is no discontinuity visible, which is an indication that there was no modehop within this scanning region.

With the piezoelectric actuator the laser can be tuned over 0.26 nm @ 780 nm (130 GHz) with a resolution of 6 MHz. Figure 10 shows the measured wavelength tuning with the piezoelectric actuator. The inset in the picture shows the power fluctuation during the piezo scan. It is in the order of 10% without any discontinuity. All measurements were done with a wavemeter (Burleigh, WA 1500) with a resolution of 60 MHz, and a calibrated power meter (Coherent, LM2). With such a configuration, we have a broad overlap for both tuning mechanisms.

The maximum scanning speed with the piezoelectric actuator is 1 kHz. Many diode laser applications require high frequency modulation of the injection current. Typical examples are lock-in measurements and noise compensation schemes, like the Pound Drever Hall stabilization for external cavity diode lasers. With this lock all acoustic vibrations or current noise induced frequency changes can be neglected. For ultra stable absorption measurement, locking to a well known wavelength reference is often necessary. Therefore, we included a high frequency bias tee within the protection circuit of our laser heads. The idea behind the use of a bias-tee is to set the laser above the threshold using a DC current source

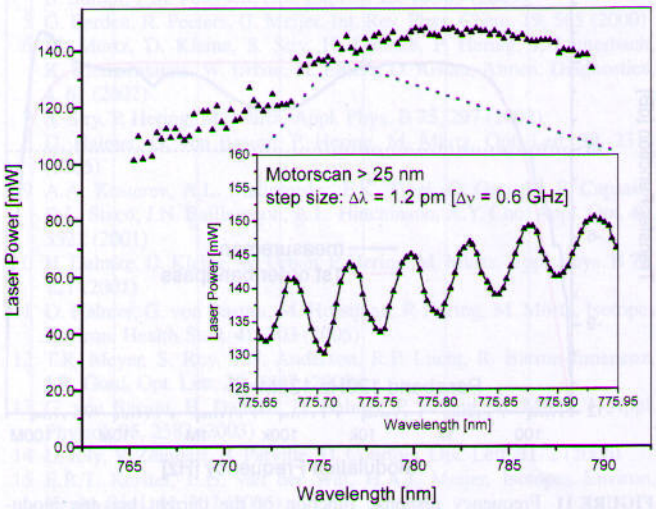

FIGURE 9 Wavelength tuning with the stepper motor. The maximum tuning range is 25 nm @ 780 nm. The *inset* shows the power modulation in detail for a smaller region. The minimal step of the servo motor is 1.25 pm

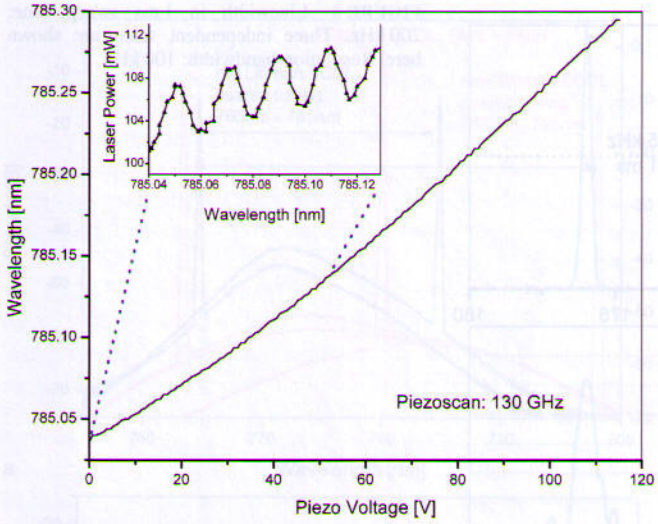

FIGURE 10 Wavelength tuning with the piezoelectric transducer. The maximal tuning range with the piezo is 130 GHz @ 780 nm. The *inset* shows the power modulation during the piezo scan

and to independently modulate the power around its average value determined by the DC current. Using the AC branch of the bias-tee (SMA), one can modulate the laser current at frequencies within the limits of the pass band. The pass band is measured and specified in the following plot in Fig. 11.

It shows a flat (±3 dB) transfer function in the modulation frequency range between 100 Hz and 100 MHz. The red line shows the behavior of an idealized bandpass. With our ECDL we measured a single mode current tuning over 5 GHz with a tuning rate of 100 kHz/mA at 10 MHz modulation frequency.

The amplitude plot is useful and sufficient for many applications, but there is another aspect. To judge the stability of feedback loops, the Nyquist–Shannon criterion demands information about the signal propagation delay (phase plot). Gain-of-one and a phase of 180° measured in an open loop are

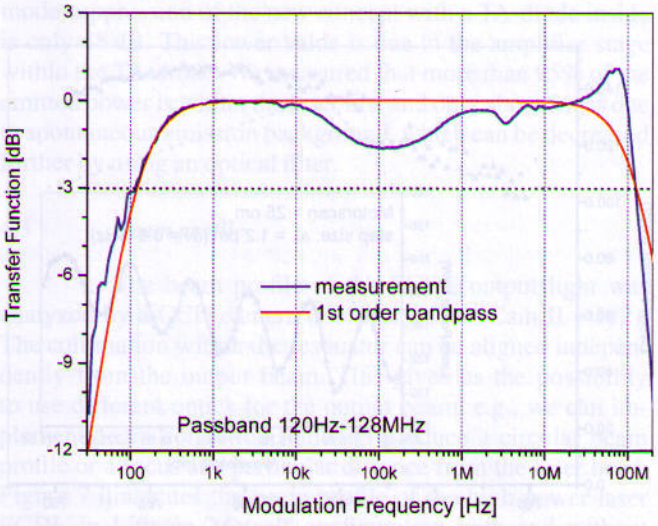

FIGURE 11 Frequency response function of the current bias-tee modulation; modulation frequency (bias-tee): 100 Hz–10 MHz, current transfer function: 20 mA/V, rf input resistance (bias-tee): 50 Ω, laser frequency response: 0.25 GHz/V, max. voltage 2 $V_{p\text{-}p}$

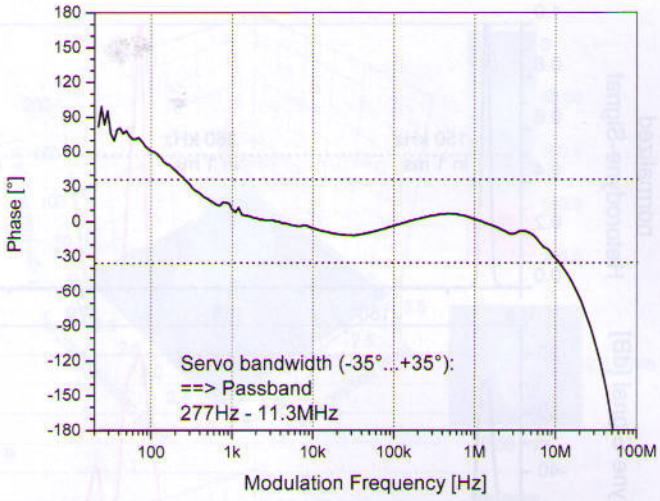

FIGURE 12 Phase plot of the bias-tee for laser current modulation

a resonance condition for the closed loop. A practical criterion for stability is the servo bandwidth defined with 35° phase difference. Figure 12 shows the phase plot of the bias-tee.

A feedback loop using our bias-tee model can be highly stable in the domain from 277 Hz to 11.3 MHz, according to the above measurement.

4.6 *Long-term stability*

The mount for the laser diode has been optimized for thermal stability. Therefore, the high power diode is soldered into a gold coated copper submount which is specially designed for high heat conductivity. The laser is mounted on a proper heat sink with a surface temperature below 28 °C.

Figure 13 pictures the measurement of the wavelength drift of the free running high power ECDL. The measurement was performed with a wavemeter (Burleigh, WA 1000), which has a resolution of 300 MHz. There was no wavelength stabilization applied to this laser at the time of measurement. These data show the excellent long-term stability due to the good thermal management.

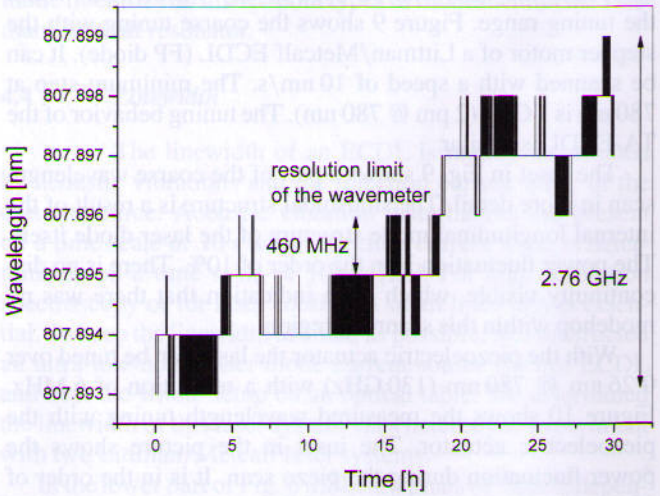

FIGURE 13 Thermal management of the high power ECDL with a drift below 2 GHz in 30 h measurement time

All these measurements show the excellent single mode tuning behavior. The combination of high power and excellent tunability in a compact setup offers the potential that such a laser system can be used in various applications. For example, such a laser should be very suitable for DFG as light source for high resolution spectroscopy or as a light source for THz generation.

4.7 *Spectroscopic application*

In order to demonstrate the suitability of this light source for high resolution spectroscopy, we tested our laser system in an ultra-sensitive CALOS spectrometer.

The capability of the high power diode laser as pump source for the DFG laser system was proved with an absorption spectrum measurement at a wavelength of 3.3 µm. In this spectral region water molecules show a characteristic fingerprint spectrum. For the absorption measurement the cavity was flushed with a sample gas mixture consisting of N_2 that was saturated with water vapor. The flow rate was controlled by an electronic mass-flow controller to be 500 cm^3/min at standard temperature and pressure conditions (1013 mbar, 272 K). In order to reduce the pressure broadening of the spectral line the pressure inside the cavity was 100 mbar. Figure 14 shows the measured water spectrum. The frequency of the DFG laser system was tuned in steps of the free spectral range of the cavity (294 MHz) via the piezoelectric transducer at the mirror inside our Littman/Metcalf ECDL.

The observed data points are shown as dots, the solid line represents the spectral line shape data from the HITRAN2000 database [23], which was fitted to the observed data. The spectrum shows water lines belonging either to the main isotopologue $H_2{}^{16}O$ or to the rare isotopologues $H_2{}^{18}O$, HDO, and $H_2{}^{17}O$. The concentration of water inside the cavity was calculated by the method of least squares with the formula $\alpha(\lambda) = c_1\alpha_1(\lambda) + \alpha_0$, where $\alpha(\lambda)$ represents the measured absorption values. In this equation $\alpha_1(\lambda)$ stands for a reference absorption spectrum, containing absorption data for the four

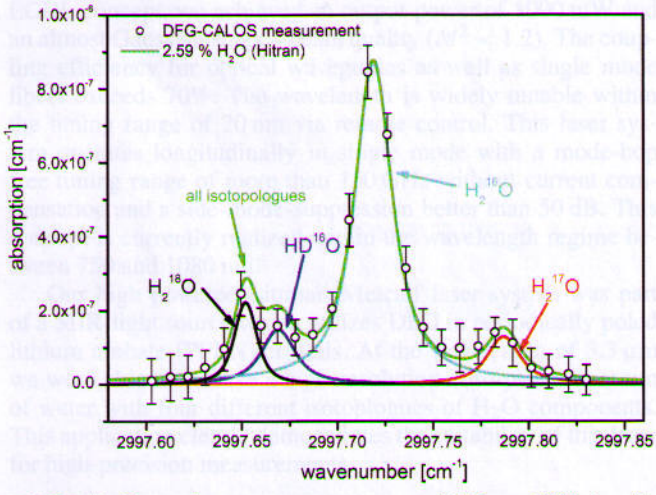

FIGURE 14 Observed water vapor spectrum at 3.335 µm. 100% humidity, 21 °C. Measured data points are shown as *open dots*; the spectral line shapes for different water isotopologues were extracted from HITRAN2000 database and are depicted as *solid lines*

water isotopologues with a natural isotope ratio, derived from the HITRAN database. With α_0 as a constant background the equation yields c_1 as a corresponding value for the measured water concentration. This calculation method is described in more detail in [9]. The concentration of water for the measurement discussed here was (2.59 ± 0.17) %. The concentration error is determined by the Gaussian error propagation with the errors of the measured absorptions.

The good agreement between the measured data points and the fitted HITRAN data shows the suitability of CALOS for isotopologue selective measurements of trace gases.

5 Conclusion

We reported on a new principle of using high power laser diodes in an external Littman/Metcalf cavity. The very compact design offers up to 1 W output power and an excellent beam propagation factor of $M^2 < 1.2$ for both axes. The laser system has a small linewidth in the 100 kHz regime and is tunable over more than 25 nm. Due to three different wavelength tuning mechanisms the laser can be automatically tuned over the complete tuning range without any discontinuities. We also demonstrated the high performance of the laser system in a CALOS experiment. This study is a proof of the high potential of the ECDL as a cost effective alternative to amplified laser systems.

ACKNOWLEDGEMENTS The CRDS experiments were performed at the infrared spectroscopy laboratory of the Institut für Lasermedizin (ILM), Universität Düsseldorf. The ILM acknowledges financial support from the Deutsche Forschungsgemeinschaft. Furthermore, S.S. and J.S. would like to thank the 'Bundesministerium für Bildung und Forschung' (BMBF) for the financial support of this work (FF 13N8062).

REFERENCES

1 L. Ricci, M. Weidenmüller, T. Esslinger, A. Hemmerich, C. Zimmermann, V. Vuletic, W. König, T.W. Hänsch, Opt. Commun. **117**, 541 (1995)
2 S. Stry, L. Hildebrandt, J. Sacher, C. Buggle, M. Kemmann, W. von Klitzing, Proc. SPIE **5336**, 17 (2004)
3 S. Stry, L. Hildebrandt, J. Sacher, Proc. SPIE **5452**, 645 (2004)
4 M. Chi, O.B. Jensen, J. Holm, C. Pedersen, P.E. Andersen, G. Erbert, B. Sumpf, P.M. Petersen, Opt. Express **13**, 10589 (2005)
5 G. Berden, R. Peeters, G. Meijer, Int. Rev. Phys. Chem. **19**, 565 (2000)
6 M. Mürtz, D. Kleine, S. Stry, H. Dahnke, P. Hering, J. Lauterbach, K. Kleinermanns, W. Urban, H. Ehlers, D. Ristau, Atmos. Diagnostics, **4**, 61 (2002)
7 S. Stry, P. Hering, M. Mürtz, Appl. Phys. B **75**, 297 (2002)
8 D. Halmer, G. von Basum, P. Hering, M. Mürtz, Opt. Lett. **30**, 2314 (2005)
9 A.A. Kosterev, A.L. Malinovsky, F.K. Tittel, C. Gmachl, F. Capasso, D.L. Sivco, J.N. Baillargeon, A.L. Hutchinson, A.Y. Cho, Appl. Opt. **40**, 5522 (2001)
10 H. Dahnke, D. Kleine, W. Urban, P. Hering, M. Mürtz, Appl. Phys. B **72**, 121 (2001)
11 D. Halmer, G. von Basum, M. Horstjann, P. Hering, M. Mürtz, Isotopes Environ. Health Stud. **41**, 303 (2005)
12 T.R. Meyer, S. Roy, T.N. Anderson, R.P. Lucht, R. Barron-Jimenenz, J.R. Gord, Opt. Lett. **30**, 3087 (2005)
13 G. von Basum, H. Dahnke, D. Halmer, P. Hering, M. Mürtz, J. Appl. Physiol. **95**, 2583 (2003)
14 L. Joly, V. Zéninari, B. Parvitte, D. Courtois, Opt. Lett. **31**, 2 (2006)
15 E.R.T. Kerstel, L.G. van der Wel, H.A.J. Meijer, Isotopes Environ. Health Stud. **41**, 207 (2005)
16 Patent No. 5867512
17 I. Shvarchuck, K. Dieckmann, M. Zielonkowski, J.T.M. Walraven, Appl. Phys. B **71**, 475 (2000)

18 J. Sacher, D. Baum, P. Panknin, W. Elsässer, E.O. Göbel, Phys. Rev. A **45**, 1893 (1992)
19 R. Lang, K. Kobayashi, IEEE J. Quantum Electron. **QE-16**, 347 (1980)
20 D. Halmer, G. von Basum, P. Hering, M. Mürtz, Rev. Sci. Instrum. **75**, 2187 (2004)
21 H. Dahnke, D. Kleine, P. Hering, M. Mürtz, Appl. Phys. B **72**, 971 (2001)
22 L. Hildebrandt, R. Knispel, S. Stry, J.R. Sacher, F. Schael, Appl. Opt. **42**, 2110 (2003)
23 HITRAN2000 database, available at http://www.hitran.com